A transcription factor-sRNA-mediated double-negative feedback loop confers pathogen-specific control of quorum-sensing genes

Authors

Ameya A. Mashruwala[1,2,3], Kaitlin Decker[1,2,5], Chenyi Fei[1,2,4], Julie Valastayan[1,2], and Bonnie L. Bassler[1,2*]

Affiliations

[1]Department of Molecular Biology, Princeton University, Princeton, New Jersey 08544, USA

[2]The Howard Hughes Medical Institute, Chevy Chase, MD 20815, USA

[3]Current address: The Stowers Institute for Medical Research, Kansas City, MO, 64110

[4]Current address: Massachusetts Institute of Technology, Cambridge, MA 02139

[5]Current address: Rutgers University, Piscataway, NJ, 08854

*Correspondence to: bbassler@princeton.edu

Abstract

The cell-to-cell communication process called quorum sensing enables bacteria to synchronize collective behaviors. Quorum sensing relies on the production, release, and detection of signaling molecules called autoinducers. In *Vibrio cholerae*, the VqmA transcription factor, following binding of the DPO autoinducer, activates expression of the gene encoding the VqmR small regulatory RNA. VqmR controls traits including biofilm formation. Here, we identify repressors of DPO-VqmA-VqmR signaling. We focus on one identified repressor, the LuxT transcription factor. We show that LuxT represses *vqmR* transcription. VqmR post-transcriptionally represses *luxT* translation. This arrangement forms a double-negative feedback loop between the two regulators. Reciprocal control hinges on the N-terminal 8 amino acids of LuxT. The nucleotide sequence encoding this LuxT region serves as the VqmR binding site in the *luxT* mRNA and the amino acids specified by this same N-terminal region are required for LuxT to bind the *vqmR* promoter. This same LuxT N-terminal region also expands the DNA motifs to which LuxT can bind. We show this regulatory circuit is unique to *V. cholerae* and closely related species and absent from other vibrios. We define the set of LuxT-controlled genes in *V. cholerae* and

show that LuxT promotes biofilm formation, a key requirement for successful colonization of eukaryotic hosts.

Importance

Bacterial quorum sensing enables control of collective behaviors. In *Vibrio cholerae*, the DPO-VqmA-VqmR quorum-sensing circuit governs key processes, including biofilm formation. Here, we identify a double-negative feedback loop between the transcription factor LuxT and the small RNA VqmR. This regulatory circuit depends on an eight amino acid N-terminal region that exists only in *V. cholerae* LuxT and LuxT from its close relatives. This short peptide sequence confers three distinct functions: It enables LuxT to repress *vqmR*, renders *luxT* mRNA susceptible to VqmR repression, and governs which DNA motifs LuxT can bind. Our findings reveal a pathogen-specific regulatory module that links small RNA targeting of mRNAs to transcription factor DNA binding specificity. The results show how evolution tailors bacterial regulatory circuits to adapt to different environments.

Introduction

Quorum sensing (QS) is a process of cell-to-cell communication that bacteria use to coordinate group behaviors (1, 2). QS involves the production, release, and population-wide detection of extracellular signal molecules called autoinducers (AIs) (1, 2). At low cell density (LCD), AI concentration is below the threshold for detection and genes required to perform individual behaviors are expressed (2, 3). As population density increases, AIs accumulate and interact with their partner receptors (2–4). AI-bound receptors drive the transition from the LCD-gene expression pattern to the high cell density (HCD) gene expression pattern, and consequently, bacteria enact group behaviors (5–10). In the human pathogen *Vibrio cholerae*, the causative agent of the cholera disease, QS regulates traits including virulence factor production and biofilm formation (11–14). Regarding *V. cholerae* biofilms, they form at LCD, and at HCD, QS represses biofilm formation and promotes biofilm dispersal (11, 15, 16).

48 *V. cholerae* possesses multiple QS systems that operate in parallel (14, 17–21). The
49 current work focuses on the QS system that relies on the AI called DPO (3,5-
50 dimethylpyrazin-2-ol), which is produced via a threonine dehydrogenase (Tdh)-
51 dependent mechanism (18). DPO is bound by the VqmA transcription factor (18). At HCD,
52 the DPO-VqmA complex activates expression of *vqmR,* encoding the VqmR small RNA
53 (sRNA) (18, 22). VqmR post-transcriptionally regulates gene expression, including
54 repressing genes required for biofilm formation (18, 22).
55
56 In addition to extracting information encoded in DPO, VqmA also acts as an information
57 processing hub that enables *V. cholerae* to integrate cues derived from the environment
58 and the human host, such as oxygen levels and bile salts (23). VqmA indirectly perceives
59 oxygen through cysteine residues that form redox-responsive disulfide bonds. In the
60 presence of both oxygen and DPO, VqmA forms a C134-C134 intermolecular disulfide
61 bond that enhances binding to the *vqmR* promoter. Indeed, the $VqmA_{C134A}$ protein, which
62 cannot form this disulfide bond, exhibits diminished DNA binding capacity (23).
63
64 Here, we perform a genetic screen to identify additional regulators of the DPO-VqmA-
65 VqmR QS circuit. We focus on the LuxT transcription factor revealed in our work. Reporter
66 and DNA binding assays demonstrate that LuxT represses *vqmR* transcription. Previous
67 work showed that *luxT* is repressed post-transcriptionally by VqmR, thus, interactions
68 between LuxT and VqmR constitute a double negative feedback loop (Figure 1, left) (22).
69 To repress *luxT* translation, the VqmR sRNA binds a 24 base pair mRNA region encoding
70 the first 8 amino acids of LuxT (22). The presence of these first 8 amino acids in the *V.*
71 *cholerae* LuxT protein has functional consequences. Specifically, *V. cholerae* LuxT can
72 bind two DNA motifs but binding to only one of these motifs, which is the motif present in
73 the *vqmR* promoter, requires that LuxT possess these N-terminal 8 amino acids. Thus,
74 operation of both negative feedback loops, VqmR repression of *luxT* and LuxT repression
75 of *vqmR*, requires the DNA encoding the first 8 amino acids of LuxT and the 8 amino acids
76 themselves, respectively. This 8-amino acid N-terminal extension is absent in LuxT
77 proteins from vibrios that are not closely related to *V. cholerae*. Therefore, non-*V. cholerae*
78 vibrios do not employ these regulatory loops (Figure 1, right). This finding raises the

79 possibility that this regulatory arrangement may be important in specific niches inhabited
80 by *V. cholerae*. Using phenotypic, genetic, and RNA-Seq analyses, we define the *V.*
81 *cholerae* LuxT-controlled regulon and show that, in addition to QS genes, LuxT regulates
82 biofilm formation and the production of metabolic enzymes.
83

84 **Results**

85 **A genetic screen in *V. cholerae* reveals repressors of DPO-VqmA-VqmR QS signal**
86 **transduction.** QS information, cues from the local environment, and human host-derived
87 stimuli are all integrated by VqmA to modulate its transcriptional activity (23). Given this
88 understanding, we wondered whether additional inputs also regulate VqmA-directed QS
89 signaling. An earlier screen revealed that VqmA activates *vqmR* expression (22). Here,
90 we carry out the opposite screen: a transposon mutagenesis screen for repressors of
91 *vqmR*. Our strategy exploited a partially impaired VqmA protein, $VqmA_{C134A}$, that exhibits
92 reduced DNA binding capacity at the *vqmR* promoter (23). Using the $VqmA_{C134A}$ allele
93 enabled us to conduct a simple, visual blue-white colony screen using a transcriptional
94 reporter in which the *vqmR* promoter drives *lacZ* expression (hereafter P*vqmR-lacZ*, with
95 the P prefix denoting promoter). Because basal P*vqmR-lacZ* activity is low in *V. cholerae*
96 carrying $VqmA_{C134A,}$ colonies are white/pale blue, unlike *V. cholerae* colonies possessing
97 wildtype (WT) VqmA, which are bright blue. We reasoned that *V. cholerae vqmA*$_{C134A}$
98 P*vqmR-lacZ* mutants that had obtained transposon insertions in genes encoding
99 repressors of DPO-VqmA-VqmR signaling would drive higher P*vqmR-lacZ* expression
100 and be identifiable as blue colonies on petri plates. Based on this logic, we mutagenized
101 Δ*tdh vqmA*$_{C134A\text{-}FLAG}$ P*vqmR-lacZ V. cholerae* and screened for blue colonies in the
102 presence of X-gal. Using a strain lacking *tdh* for the screen ensured that hits would be
103 restricted to genes encoding components that act on signal relay (*vqmA* or *vqmR*) not
104 signal production (*tdh*). We did not supply DPO during the screen. The strategy was to
105 keep the endogenous P*vqmR-lacZ* activity as low as possible to enhance detection of
106 insertion mutants exhibiting even modest increases. We assessed ~20,000 colonies and
107 identified transposon insertions in 14 genes, which encoded 6 regulatory proteins, 4
108 components involved in transport and metabolism, and 4 genes with undefined functions.
109

110 To confirm the hits from our screen, we engineered P*vqmR-lux* as a reporter to quantify
111 *vqmR* promoter activity (22, 23). We introduced the P*vqmR-lux* fusion onto the
112 chromosomes of Δ*tdh V. cholerae* possessing either *vqmA*$_{FLAG}$ or *vqmA*$_{C134A\text{-}FLAG}$. In the
113 absence of DPO, P*vqmR-lux* activity was ~27-fold higher in the Δ*tdh vqmA*$_{FLAG}$ strain than
114 in the Δ*tdh vqmA*$_{C134A\text{-}FLAG}$ strain, showing that VqmA$_{C134A\text{-}FLAG}$ is, as expected, impaired
115 in activity. Supplementation with DPO increased *vqmR-lux* activity ~4-fold in the Δ*tdh*
116 *vqmA*$_{FLAG}$ strain and ~37-fold in the Δ*tdh vqmA*$_{C134A\text{-}FLAG}$ strain (Figure 2A and B,
117 respectively). Thus, the P*vqmR-lux* reporter responds properly to DPO-mediated VqmA
118 activation, and exploiting the VqmA$_{C134A\text{-}FLAG}$ mutant expands the dynamic range of the
119 AI response assay.
120
121 To verify that components identified in our screen influence DPO-VqmA-VqmR signaling,
122 we deleted each of the identified genes from the chromosome of the Δ*tdh vqmA*$_{C134A\text{-}FLAG}$
123 P*vqmR-lux V. cholerae* strain. Deletions of four of the candidate genes, *vc0122, vc2614,*
124 *vca0566,* and *vca0917* resulted in 9-, 13.5-, 2.8-, and 3.3-fold increases in P*vqmR-lux*
125 activity, respectively (Figure 2C). Additional temporal differences occur across strains. For
126 simplicity, here, we focus on maximal fold changes. The remaining ten genes did not
127 significantly alter P*vqmR-lux* output (Figure S1). It is possible that these ten genes were
128 false positives or that they only influence *vqmR* expression on solid medium, etc. We did
129 not study them further. The remainder of the present work is focused on *vc0122, vc2614,*
130 *vca0566,* and *vca0917*. These genes encode Acy, Crp, WigR, and LuxT, respectively.
131
132 **LuxT represses *vqmR* transcription.** The putative repressors identified in our screen
133 could decrease DPO-VqmA-VqmR signaling by repressing expression of either *vqmA* or
134 *vqmR*. To distinguish between these two possibilities, we engineered a Δ*tdh* Δ*vqmA V.*
135 *cholerae* strain carrying P$_{BAD}$-*vqmA* at a neutral chromosomal locus. The strain also
136 harbors the chromosomal P*vqmR-lux* fusion. We refer to this strain simply as the P$_{BAD}$-
137 *vqmA* strain. We introduced deletions of *acy*, *crp*, *wigR*, and *luxT* into the P$_{BAD}$-*vqmA*
138 strain and measured P*vqmR-lux* output. Our rationale is as follows: VqmA is required to
139 activate *vqmR* expression. In the P$_{BAD}$-*vqmA* strain, following the addition of arabinose,
140 VqmA is produced and activates P*vqmR-lux*. Since *vqmA* is driven by a synthetic

141 promoter, it is not subject to native regulation. Thus, if deletion of a gene(s) identified in
142 our screen results in increased P*vqmR-lux* activity, then *vqmR* must be the target of that
143 particular repressor. By contrast, if no change in P*vqmR-lux* occurs, then we can infer
144 that repression must occur through changes in *vqmA* transcription, VqmA activity, or
145 VqmA turnover. Figure 3A shows that deletion of *crp* and *luxT* from the P_{BAD}-*vqmA* strain
146 resulted in ~13.2-fold and 2.5-fold increases in P*vqmR-lux* activity suggesting that *crp*
147 and *luxT* modulate VqmR levels. By contrast, no change in P*vqmR-lux* activity occurred
148 when *acy* and *wigR* were deleted, suggesting they modify *vqmA* expression or VqmA
149 abundance or activity. We quantified $VqmA_{FLAG}$ abundance in the Δ*tdh V. cholerae* strain
150 when *acy* or *wigR* was deleted. We note that, here, $vqmA_{FLAG}$ is driven by its endogenous
151 promoter. We used the Δ*tdh* Δ*crp* and Δ*tdh* Δ*luxT* strains as controls for comparison. Our
152 logic was that if Acy and WigR modify *vqmA* transcription or VqmA abundance, then in
153 the Δ*acy* and Δ*wigR* strains, VqmA levels would differ from those in the parent strain.
154 Neither mutant displayed any change in $VqmA_{FLAG}$ abundance (Supplementary Figure 2).
155 Thus, Acy and WigR apparently modulate VqmA activity by a post-translational
156 mechanism(s).
157
158 *acy* and *crp* encode adenylate cyclase (Acy) and the cAMP receptor protein (Crp),
159 respectively. Acy and Crp typically function together (24–26). Acy synthesizes cAMP,
160 which is bound by Crp. The Crp-cAMP complex regulates transcription of target genes,
161 particularly those involved in utilization of different carbon sources. Given this well-
162 established partnership, it is surprising that we find that Acy and Crp apparently work
163 independently of each other to control the DPO-VqmA-VqmR QS circuit with Acy affecting
164 VqmA activity, and Crp modifying P*vqmR* expression. *V. cholerae* possesses at least two
165 additional Crp family proteins, neither of which have been studied. One or both of them
166 could partner with Acy to regulate VqmA activity. WigR is a response regulator that, with
167 its partner kinase WigK, constitutes a two-component system that is proposed to monitor
168 cell wall damage (27, 28). Our finding suggests the possibility that cell wall damage feeds
169 into QS control of gene expression.
170

171 For the remainder of this study, we characterize the role of LuxT in *vqmR* regulation. *V.*
172 *cholerae* LuxT (LuxT$_{Vc}$) is a transcription factor, the mRNA of which was previously
173 identified as a direct target of repression by the VqmR sRNA (22). Our identification of
174 LuxT$_{Vc}$ as a repressor of *vqmR* suggests that VqmR and LuxT$_{Vc}$ constitute a double-
175 negative feedback loop.
176
177 To probe whether LuxT regulates *vqmR* by transcriptional repression, we analyzed the
178 *vqmR* promoter for a consensus LuxT binding sequence. *Vibrio harveyi* LuxT (LuxT$_{Vh}$)
179 shares 75% amino acid identity with LuxT$_{Vc}$, making it likely that both proteins bind similar
180 DNA sequences. A prior study in *V. harveyi* identified a LuxT (LuxT$_{Vh}$) binding site in the
181 promoter of *swrZ* (29). Indeed, inspection of the *V. cholerae vqmR* promoter (P*vqmR*$_{Vc}$)
182 revealed a potential LuxT binding site located at -28 to -9 upstream of the *vqmR*$_{Vc}$
183 transcriptional start site. To determine if LuxT$_{Vc}$ binds this motif, we purified 6X-His-LuxT$_{Vc}$
184 and combined it in an electrophoretic mobility shift assay (EMSA) with a probe containing
185 *V. cholerae* P*vqmR*$_{Vc}$ (-111 to +49) or, as a control, the same probe containing a
186 scrambled version of the putative LuxT binding sequence (P*vqmR*$_{Vc\ \mathrm{scrambled}}$) (Figure 3B).
187 6X-His-LuxT$_{Vc}$ bound to *PvqmR*$_{Vc}$ but not *PvqmR*$_{Vc\ \mathrm{scrambled}}$, suggesting that LuxT directly
188 represses *vqmR* expression (Figure 3B). We refer to the LuxT binding motif in P*vqmR*$_{Vc}$
189 as Motif 1. Since we already know that the VqmR sRNA represses *luxT*, we conclude that
190 LuxT and VqmR interact in a double-negative feedback loop.
191
192 **LuxT-VqmR feedback loops are present only in *V. cholerae* and *V. cholerae*-like**
193 **vibrio species.** Given that both LuxT and VqmR are present across vibrios, we wondered
194 whether their regulatory interactions are likewise conserved across the genus. Using
195 bioinformatic analyses, we compared the DNA sequences encoding P*vqmR* and the *luxT*
196 region targeted by *vqmR* from representative strains across sequenced vibrio species.
197
198 First, we discuss LuxT repression of P*vqmR*. Vibrio P*vqmR* sequence comparisons are
199 shown in a pair-wise sequence similarity color-map (Figure 4A, blue indicating highest
200 similarity). We compared a 50-nucleotide region from -48 to +2 relative to the *vqmR*
201 transcriptional start site. This sequence space contains 20 nucleotides corresponding to

202 the $LuxT_{Vc}$ binding site (-28 to -9), together with 20 upstream and 10 downstream
203 nucleotides. We analyzed one representative genome across sixty-three different vibrios
204 that harbor both *luxT* and *vqmR*. For simplicity, only the LuxT consensus binding site is
205 shown in the figure, and it varies across P*vqmR* sequences. To test LuxT tolerance for
206 variation in binding site, we chose a few similar and quite different putative LuxT binding
207 sites from the set of *vqmR* promoters and performed EMSA analyses using 6X-His-
208 $LuxT_{Vc}$. The test sites come from P*vqmR* in *Vibrio metoecus*, *Vibrio splendidus*, and *V.*
209 *harveyi* (denoted $PvqmR_{Vm}$, $PvqmR_{Vs}$, and $PvqmR_{Vh}$, respectively, and are displayed in
210 Figure 4A). The *V. cholerae* and *V. metoecus* P*vqmR* sequences are in the same cluster
211 as the site bound by $LuxT_{Vc}$ in $PvqmR_{Vc}$, differing by only 3 base pairs (sequence
212 differences are highlighted in red in Figure 4A). Not surprisingly, like $PvqmR_{Vc}$, $LuxT_{Vc}$
213 bound $PvqmR_{Vm}$ (Figure 4B). By contrast, the LuxT binding sequences from *V. splendidus*
214 and *V. harveyi*, which differ from that in $PvqmR_{Vc}$ by ~40-50%, were not bound by $LuxT_{Vc}$
215 (Figure 4B). These findings suggest that LuxT repression of P*vqmR* occurs only in *V.*
216 *cholerae* and closely related vibrios.
217
218 Now we discuss VqmR repression of *luxT*. We have previously shown that the VqmR
219 sRNA binds to a 24 base pair region encoding the first 8-amino acids of $LuxT_{Vc}$ (22). To
220 determine whether this N-terminal 8 amino acid extension is present in other vibrio LuxT
221 proteins, we compared this 24-base pair region in *luxT* DNA sequences across vibrio
222 genomes. A pair-wise sequence similarity color-map shows that the DNA sequences
223 across vibrio *luxT* genes roughly separate into two clusters: one resembling *V. cholerae*
224 and the other resembling *V. harveyi* (Figure 4C). Notably, the *V. cholerae* start codon
225 (TTG) in the *luxT* sequence is absent in vibrios that are not closely related to *V. cholerae*
226 (Figure 4C). Rather, in *V. harveyi* and its relatives, *luxT* transcription is predicted to initiate
227 at a downstream, ATG start codon. Consequently, we predict that *V. harveyi* $LuxT_{Vh}$ and
228 vibrios in the $LuxT_{Vh}$ cluster will produce a shorter LuxT isoform that lacks the 8 N-terminal
229 amino acids present in *V. cholerae* LuxT. These findings imply that VqmR might only
230 repress production of $LuxT_{Vc}$ but not LuxT in vibrios that contain LuxT proteins that cluster
231 with $LuxT_{Vh}$.
232

233 **The N-terminal 8 amino acids in *V. cholerae* LuxT expand the DNA motifs to which**
234 **LuxT can bind.** Our bioinformatic results suggest that the 24 base pair region encoding
235 the first 8 amino acids of $LuxT_{Vc}$ is specific to *V. cholerae*. We wondered whether having
236 that N-terminal amino acid extension is accompanied by functional consequences on the
237 ability of $LuxT_{Vc}$ to bind DNA. To explore this idea, we purified 6X-His-$LuxT_{Vc}$ and 6X-His-
238 $LuxT_{Vc\ \Delta 8\text{-AA N-term}}$, which lacks the first 8 N-terminal amino acids, and tested binding to
239 P*vqmR*$_{Vc}$. As expected, the probe was bound by $LuxT_{Vc}$, however, $LuxT_{Vc\ \Delta 8\text{-AA N-term}}$
240 displayed minimal binding (Figure 5A). These results show that the first 8 amino acids in
241 $LuxT_{Vc}$ are essential for binding to P*vqmR*$_{Vc}$. We also examined whether the absence of
242 the first eight amino acids in LuxT affected binding at other target DNA promoter
243 sequences. As mentioned, in *V. harveyi*, $LuxT_{Vh}$ regulates *swrZ* (P*swrZ*$_{Vh}$) encoding a
244 GntR type transcriptional regulator. As no LuxT-controlled genes other than *vqmR* were
245 known in *V. cholerae*, we assessed $LuxT_{Vc}$ binding to P*swrZ*$_{Vh}$ as a surrogate (see note
246 on a newly identified *V. cholerae* LuxT-controlled gene, *hapR*, in the Discussion). Both
247 $LuxT_{Vc}$ and $LuxT_{Vc\ \Delta 8\text{-AA N-term}}$ bound with similar affinities to P*swrZ*$_{Vh}$, demonstrating that
248 while the first 8 amino acids of LuxT are necessary to bind P*vqmR*$_{Vc}$, they are dispensable
249 for binding to P*swrZ*$_{Vh}$ (Figure 5B, left). Below, we explore $LuxT_{Vc}$ regulation of *V. cholerae*
250 genes beyond *vqmR*.
251
252 Inspection of P*swrZ*$_{Vh}$ for potential LuxT binding sites reveals a sequence located
253 between -30 to -7 upstream of the *swrZ*$_{Vh}$ start codon with some similarity to Motif 1 in
254 P*vqmR*$_{Vc}$ (Figure 5). Indeed, an EMSA probe spanning -110 to +20 (P*swrZ*$_{Vh\ \text{-110 to +20}}$),
255 that includes the Motif 1-like sequence, is bound by both $LuxT_{Vc}$ and $LuxT_{Vc\ \Delta 8\text{-AA N-term}}$.
256 Surprisingly, randomizing the Motif 1-like sequence in P*swrZ*$_{Vh}$ (P*swrZ*$_{Vh\ \text{-110 to +20 Motif 1-like}}$
257 $_{\text{scrambled}}$, Figure 5B, right) did not alter $LuxT_{Vc}$ and $LuxT_{Vc\ \Delta 8\text{-AA N-term}}$ binding, suggesting
258 that both LuxT isoforms do not bind this Motif 1-like sequence, but rather recognize a
259 sequence in P*swrZ*$_{Vh}$ that is distinct from that present in P*vqmR*$_{Vc}$.
260
261 To pinpoint the sequence in the -110 to +20 P*swrZ*$_{Vh}$ probe that is bound by $LuxT_{Vc}$, we
262 assayed seven overlapping fragments that span this region (Supplementary Figure 3).
263 Notably, two fragments containing only the Motif 1-like and immediate flanking sequences

264 (probes -40 to -6 and -30 to +20, Supplementary Figure S3) were not bound by $LuxT_{Vc}$.
265 Rather, the binding profiles show that a 25-nucleotide region residing at -75 to -51 relative
266 to the $swrZ_{Vh}$ start codon is bound by $LuxT_{Vc}$. We refer to this sequence as Motif 2
267 ($PswrZ_{Vh\ -75\ to\ -51}$; Figure 5C-D and Supplementary Figure S3). This sequence (5'-
268 CATAATCAGTACGCTGTATTATCAA-3') does not exist in $PvqmR_{Vc}$. The probe with the
269 Motif 2 sequence is also bound by $LuxT_{Vc\ \Delta 8\text{-}AA\ N\text{-}term}$ (Figure 5C). Importantly, scrambling
270 this sequence ($PswrZ_{Vh\ -75\ to\ -51\ Motif\ 2\ scrambled}$) eliminated binding by both LuxT proteins
271 (Figure 5C). Thus, $LuxT_{Vc}$ recognizes two different motifs (Figure 5D). Since $LuxT_{Vc\ \Delta 8\text{-}AA}$
272 $_{N\text{-}term}$ bound $PswrZ_{Vh}$, the N-terminal 8 amino acids are dispensable for $LuxT_{Vc}$ to
273 recognize Motif 2 present in $PswrZ_{Vh}$. We conclude that the inclusion of the first 8 N-
274 terminal amino acids in LuxT expands the possibilities for *V. cholerae* LuxT to control
275 gene expression by enabling binding to at least two distinct motifs.
276
277 **$LuxT_{Vc}$ promotes biofilm formation in *V. cholerae* at LCD.** A previous RNA-Seq study
278 in *V. harveyi* identified that the $LuxT_{Vh}$ regulon includes *swrZ* and ~10 genes specifying
279 GGDEF or EAL domain-containing proteins that synthesize and degrade, respectively,
280 the second messenger c-di-GMP molecule (29). In *V. cholerae,* c-di-GMP levels influence
281 biofilm formation (30, 31). Thus, we wondered whether $LuxT_{Vc}$ regulates biofilm formation.
282 To assess this possibility, we monitored colony biofilm morphologies of the *V. cholerae*
283 Δ*tdh* and Δ*tdh* Δ*luxT* strains. In *V. cholerae*, biofilm formation drives a change in colony
284 appearance from smooth to wrinkled, with the latter coinciding with an increase in colony
285 height (32–35). Thus, three-dimensional colony height profiles track with biofilm
286 formation. Both the Δ*tdh* and Δ*tdh* Δ*luxT* strains failed to form biofilms, with colonies only
287 reaching heights of ~100 μm (Figure 6).
288
289 The master HCD QS regulator HapR is a key repressor of *V. cholerae* biofilm formation
290 (11, 30). Thus, we reasoned that $LuxT_{Vc}$-dependent biofilm phenotypes might be revealed
291 in the absence of *hapR*. Indeed, Figure 6 shows that while the Δ*tdh* Δ*hapR* strain formed
292 colony biofilms with heights reaching up to ~550 μm, heights of Δ*tdh* Δ*hapR* Δ*luxT*
293 colonies reached only ~250 μm. Thus, *V. cholerae* forms colony biofilms only in the
294 absence of HapR and, in this LCD context, $LuxT_{Vc}$ promotes biofilm formation.

295

296 Production of the VqmR sRNA at HCD suppresses colony biofilm formation (18, 22). To
297 probe whether $LuxT_{Vc}$ modulates biofilm formation via control of *vqmR*, we compared
298 colony morphologies of the Δ*tdh* Δ*hapR* Δ*vqmA* and Δ*tdh* Δ*hapR* Δ*vqmA* Δ*luxT* strains.
299 VqmA is required for activation of $P_{vqmR_{Vc}}$, thus in its absence, *vqmR* is not expressed
300 (22). The Δ*tdh* Δ*hapR* Δ*vqmA* strain formed colony biofilms similar to those of the Δ*tdh*
301 Δ*hapR* strain with heights reaching up to ~550 μm, while colony biofilms of the Δ*tdh*
302 Δ*hapR* Δ*vqmA* Δ*luxT* strain had heights of ~250 μm (Figure 6). Thus, in our assays,
303 endogenous levels of VqmA and VqmR do not influence colony biofilm formation so
304 $LuxT_{Vc}$ must drive biofilm formation by a mechanism that is independent of VqmA and
305 VqmR.
306

307 **$LuxT_{Vc}$ controls a regulon of *V. cholerae* genes at HCD.** Given that $LuxT_{Vc}$ binds to
308 distinct DNA motifs and it regulates *V. cholerae* biofilm formation independently of VqmA-
309 VqmR, we reasoned that $LuxT_{Vc}$ may control additional genes. To define the *V. cholerae*
310 $LuxT_{Vc}$-controlled regulon, we conducted RNA-Seq on the *V. cholerae* Δ*tdh* Δ*luxT* strain
311 carrying plasmid-borne $luxT_{Vc}$ under control of the arabinose promoter (P_{BAD}-$luxT_{Vc}$).
312 Following growth to HCD in the presence and absence of arabinose, approximately 20
313 genes displayed changes in expression of >2-fold (Figure 7). As anticipated, $luxT_{Vc}$ was
314 the most upregulated gene in the dataset. Other $LuxT_{Vc}$-regulated genes included ones
315 involved in galactose and sulfate metabolism, which were activated and repressed ~2-4
316 fold, respectively. Alteration of expression of a gene specifying an orphan histidine kinase
317 (*vc1088*, ~3-fold) occurred. *vc1088* resides immediately adjacent to an 8-gene operon
318 (*vc1080*-*vc1087*) encoding genes involved in nitric oxide sensing and biofilm formation
319 (36–38). Additionally, several genes specifying hypothetical proteins or those with
320 domains of unknown function were differentially expressed. Other than *vc1088*, which,
321 given its genomic context, we hypothesize is a regulator of biofilm genes, the regulon did
322 not harbor genes known to be involved in biofilm formation. This result was expected
323 because the strain used in the RNA-Seq experiment possesses HapR, and as shown in
324 Figure 6, HapR represses biofilm formation at HCD. Also, as expected, we did not identify
325 *vqmR* because our sample preparation was not optimized for enrichment of small RNAs.

The RNA-Seq data, together with the other findings from the above studies, suggest that LuxT acts broadly to regulate signaling and metabolic pathways in *V. cholerae*, ranging from QS to biofilm formation to sulfate metabolism.

Discussion:

Here, we used a genetic screen to identify repressors of the *V. cholerae* DPO-VqmA-VqmR QS circuit. Our screen revealed four genes; *acy*, *crp*, *wigR*, and *luxT*. We focused on understanding the role of LuxT, a TetR-family transcriptional regulator, in control of the DPO-VqmA-VqmR QS circuit. TetR-family proteins frequently bind small-molecule ligands and a target DNA motif (39). We demonstrate that *V. cholerae* LuxT binds DNA; it remains to be determined whether it binds a ligand. *luxT* is conserved across vibrio species. In *V. harveyi*, LuxT represses expression of the gene encoding the small QS regulatory RNA called Qrr1 at LCD, a function conserved in several vibrio species but not in *V. cholerae* (40). By contrast, we show that in *V. cholerae*, LuxT represses expression of the gene encoding the VqmR small RNA, and this feature is not conserved in *V. harveyi.* Thus, as a broader regulatory theme, LuxT represses genes encoding sRNAs that function at the hearts of QS systems. In the context of LuxT regulation of QS components, we note that, after we concluded our experiments, a study was published reporting that $LuxT_{Vc}$ binds $P_{hapR_{Vc}}$. The motif identified is similar to that in $P_{vqmR_{Vc}}$ (Figure 5D) (41).

Our findings also reveal that VqmR post-transcriptionally represses LuxT by targeting the mRNA region encoding its first eight amino acids. The eight N-terminal amino acid residues are required for LuxT to bind the *vqmR* promoter. Furthermore, while $LuxT_{Vc\ \Delta 8\text{-}AA\ N\text{-}term}$ fails to bind the *vqmR* promoter, it nonetheless retains binding to another promoter, P*swrZ*. LuxT in other vibrios lacks this N-terminal extension. We propose that the acquisition of the LuxT N-terminal 8 amino acids delivers three activities: it allows repression of *luxT* by VqmR, it enables LuxT binding to the *vqmR* promoter to establish the VqmR-LuxT double-negative feedback loop, and it promotes regulon expansion by broadening the DNA motifs to which LuxT can bind (Figure 1). To our knowledge, this is the first example in which the mRNA sequence that is targeted by a sRNA regulator encodes a portion of a protein that governs that protein's DNA-binding capabilities.

357

358 Double negative feedback loops are common in biological systems requiring tight
359 regulation of state transitions. For instance, in bacteriophage λ, the cI and Cro proteins
360 mutually repress each other to control the switch between lysogenic and lytic cycles (42).
361 Similarly, in *Sinorhizobium meliloti*, a double negative feedback loop between the NtrBC
362 two-component system and the small RNA NfeR1 modulates nitrogen metabolism (43).
363 In *V. cholerae*, the transition from LCD to HCD QS modes involves upregulation of genes
364 encoding energetically costly processes such as motility and the type six secretion system
365 (7, 44, 45). Thus, the double negative feedback between LuxT and VqmR may serve as
366 a buffer that prevents inappropriate transitions between states until conditions are
367 optimal.

368

369 In *V. cholerae*, we find that LuxT promotes biofilm formation in a strain genetically locked
370 into expressing LCD QS behaviors. The mechanism by which LuxT mediates this effect
371 remains undefined but is independent of HapR. Preliminary analyses of promoter regions
372 of canonical biofilm genes do not reveal recognizable LuxT binding motifs, raising the
373 possibility that LuxT binds to an uncharacterized DNA sequence in these promoters or,
374 alternatively, it indirectly regulates biofilm formation genes. That LuxT regulates biofilm
375 formation is particularly intriguing in light of recent work in *V. harveyi*, where LuxT was
376 shown to be a global regulator of gene expression at LCD (29, 40). Here, we primarily
377 characterized LuxT functions in *V. cholerae* at HCD. Studies to identify the full *V. cholerae*
378 LuxT regulon across different cell densities are required to delineate the scope of its
379 regulatory roles.

380

381 Biofilm formation is required for *V. cholerae* to colonize the anaerobic intestinal lumen of
382 infant mice and to form communities on human host cells (41, 46–48). Given that *luxT*
383 and the DPO-VqmA-VqmR QS circuit are responsive to oxygen levels and human-host
384 produced bile salts, future studies could examine the roles of LuxT, the DPO-VqmA-VqmR
385 QS circuit, and the VqmR-LuxT double negative feedback during the *V. cholerae*
386 infectious lifecycle (23, 41).

387

388 **Materials and Methods:**

389 **Bacterial growth, strain construction and reagents.** *Escherichia coli* Top10 and
390 *Saccharomyces cerevisiae* were used as hosts for cloning, while *E. coli* S17-1 λ*pir* was
391 used for conjugations. Cultures of *V. cholerae* and *E. coli* were grown in LB medium at
392 37°C with shaking. When required, media were supplemented with streptomycin, 200
393 µg/mL; kanamycin, 50 µg/mL; polymyxin B, 50 µg/mL; chloramphenicol, 1 µg/mL;
394 spectinomycin, 200 µg/mL. Bioluminescence-reporter assays were conducted as
395 previously described (23). Where indicated, relative light units (RLU) denote
396 bioluminescence output divided by the culture optical density.

397

398 Chromosomal alterations were introduced into *V. cholerae* using multiplexed genome
399 editing (MuGENT) or the pRE112 suicide vector harboring the counter-selectable *sacB*
400 gene as previously described (23, 49). Unless otherwise specified, chromosomal DNA
401 from *V. cholerae* C6706 was used as the template for PCR reactions. Plasmids were
402 constructed using pBAD-pEVS or pRE112 as backbones and assembled using NEB Hi-
403 Fi reagent or yeast-recombination-assisted assembly as previously described (50).
404 Strains, plasmids, and oligonucleotides used in the study are listed in Supplementary
405 Tables 1, 2, and 3, respectively.
406 Gel purification and plasmid preparation kits, iProof DNA polymerase, and
407 Deoxynucleotide Mix were purchased from Qiagen, Bio-Rad, and New England Biolabs,
408 respectively.

409

410 **Sequence analyses.** Sequence-similarity based identification of *luxT* and *vqmR* genes
411 across vibrio genomes has been described (40, 51). A custom MATLAB (MathWorks;
412 2022) algorithm was used to search for *luxT* and *vqmR* genes in the genomes of 134
413 vibrio strains, each representing a distinct species. The initial search identified 63 vibrio
414 species harboring both *luxT* and *vqmR* genes. We further analyzed these species for
415 sequence conservation within each gene as well as their promoters. Multiple sequence
416 alignments were performed and the output analyzed in MATLAB. A standard scoring
417 matrix NUC44 (see ftp.ncbi.nih.gov/blast/matrices/) was used to compute similarity

418 scores between DNA sequences. The unweighted pair group method with arithmetic
419 mean (UPGMA) was subsequently used to cluster vibrio species with similar sequences.
420
421 **Protein purification.** Genes encoding 6X-His-tagged proteins were cloned into pET15b
422 and transformed into *Escherichia coli* BL21. Strains for protein production were cultured
423 in LB with 100 µg/mL ampicillin and incubated at 37°C with aeration. When cultures
424 reached an OD_{600} of 0.5, 400 µM IPTG was added to induce protein production. The
425 cultures were further incubated at 18°C overnight. Cells were harvested via centrifugation
426 at 4,000 rpm for 10 min. The resulting cell pellets were resuspended in 1/100 volume of
427 lysis buffer (50 mM Tris-HCl, 150 mM NaCl, pH 8) containing 5 µM benzonase, 3 µM
428 imidazole, 250 µg/mL lysozyme, and BugBuster Protein Extraction Reagent (Novagen).
429 The lysate was subjected to centrifugation at 13,000 rpm for 20 min, and the clarified
430 supernatant was combined with Ni-NTA Superflow resin (Qiagen) equilibrated with 3 µM
431 imidazole. After allowing the resin and protein to incubate for 1 h at 4°C, the resin was
432 subjected to a series of washes with imidazole at concentrations from 3 µM to 40 µM.
433 Protein was eluted from the resin with buffer (50 mM Tris-HCl, 150 mM NaCl, pH 8)
434 containing 300 µM imidazole. Purified protein was dialyzed overnight at 4°C with Slide-A-
435 Lyzer modules (Thermo Fisher) in buffer (50 mM Tris-HCl, 150 mM NaCl, pH 8),
436 concentrated, flash-frozen, and stored at -80°C.
437
438 **Electromobility gel shift assays (EMSAs).** DNA probes were purchased as G-Blocks
439 from IDT (~200 base pairs) and were used as templates for PCR amplification. The
440 resulting PCR products were gel purified using the QIAquick PCR Purification kit
441 (Qiagen), eluted with sterile water, and stored at 4° C until use. Alternatively, duplex DNA
442 oligomers (~20-30 base pairs) were purchased from IDT and used in assays. To initiate
443 EMSA assays, 0.6 to 6 µM of purified protein in buffer (50 mM Tris-HCl, 150 mM NaCl,
444 pH 8) was combined with DNA probes normalized to 5-15 ng. Mixtures were reacted for
445 20 min at room temperature and subsequently subjected to electrophoresis on Novex 6%
446 DNA Retardation Gels (Thermo Fisher) in 1X Tris-buffered EDTA (TBE) at 4°C (23). DNA
447 probes were visualized with Sybr Green stain (Thermo Fisher) and imaged with an
448 ImageQuant 800 imaging system (Cytiva) (23).

449

450 **Immunoblotting**. *V. cholerae* strains were cultured overnight in M9 minimal medium. The
451 next day, the cultures were diluted 1:1000 into fresh M9 medium containing 0.01%
452 arabinose and grown to an OD_{600} of 1. Cells were pelleted by centrifugation and
453 resuspended in 20 µL of ice-cold phosphate-buffered saline (PBS) at an OD_{600} of 3.5.
454 Cells were lysed, protein extracts were separated on SDS-PAGE gels, and
455 immunoblotting was performed as described previously (23). Protein levels were
456 assessed using ImageJ software.

457

458 **Biofilm assays and image analyses.** *V. cholerae* strains were cultured overnight in LB
459 medium at 37°C with aeration. Cultures were subjected to vortex for 5 min with 4 mm
460 glass beads added to disrupt cell aggregates. The samples were diluted to OD_{600} = 0.5 in
461 1X PBS. The cultures were again subjected to vortex for 5 min without beads. 1 µL of
462 each culture was spotted onto an LB plate containing 50 mg/mL polymyxin B. When
463 strains carried plasmids, plates contained 40 mg/mL polymyxin B, 25 mg/mL kanamycin,
464 and, when specified, 0.01% arabinose. The plates were incubated at 37°C and biofilms
465 were imaged every 24 h with a Leica M125 stereomicroscope. Colony height profiles were
466 captured using a Keyence VK-X3000 laser microscope (32). Images were analyzed using
467 the manufacturer provided MultiFileAnalyzer application. Lateral topographic cross
468 sections were profiled in triplicate. For each cross section, the program identified the
469 minimum and maximum heights.

470

471 **RNA sequencing**. Overnight cultures of *V. cholerae* were diluted to OD_{600} = 0.0025 and
472 grown to OD_{600} = 0.05 in LB. Cultures were divided in half: 0.1% arabinose was
473 administered to one half and the other half received LB as a control. The treated cultures
474 were grown to OD_{600} = 0.25. RNA Protect solution (Qiagen) was added at 2:1 v/v
475 reagent:culture and RNA was purified using the RNeasy Mini Kit (Qiagen) followed by
476 treatment with DNase (Ambion AM 1907) using the manufacturers' recommended
477 procedures with minor modifications are described previously (7). RNA samples were
478 sequenced by SeqCenter (Pittsburgh, PA).

479

Acknowledgments:

We thank Bassler group members for thoughtful discussions. This work was supported by the Howard Hughes Medical Institute, NSF grant MCB-2508324, and NIH grant 5R37GM065859 to B.L.B. A.A.M. was supported as a Howard Hughes Medical Institute Fellow of the Life Sciences Research Foundation and, subsequently, as a member of the Stowers Institute for Medical Research.

This manuscript is the result of funding in whole or in part by the National Institutes of Health (NIH). It is subject to the NIH Public Access Policy. Through acceptance of this federal funding, NIH has been given a right to make this manuscript publicly available in PubMed Central upon the Official Date of Publication, as defined by NIH.

Author contributions:

A.A.M, K.D., J.V., C.F., and B.L.B designed experiments and analyzed data; A.A.M, K.D., and J.V. constructed strains and performed wet-lab experiments; C.F., A.A.M, and B.L.B designed bioinformatic experiments and C.F. performed bioinformatic experiments and analyses; K.D., C.F., and A.A.M, wrote custom scripts for data analyses and visualization; A.A.M, K.D., and B.L.B wrote the original draft; A.A.M, K.D., J.V., C.F., and B.L.B reviewed and edited subsequent manuscript versions. B.L.B provided oversight, resources, and funding.

Figures:

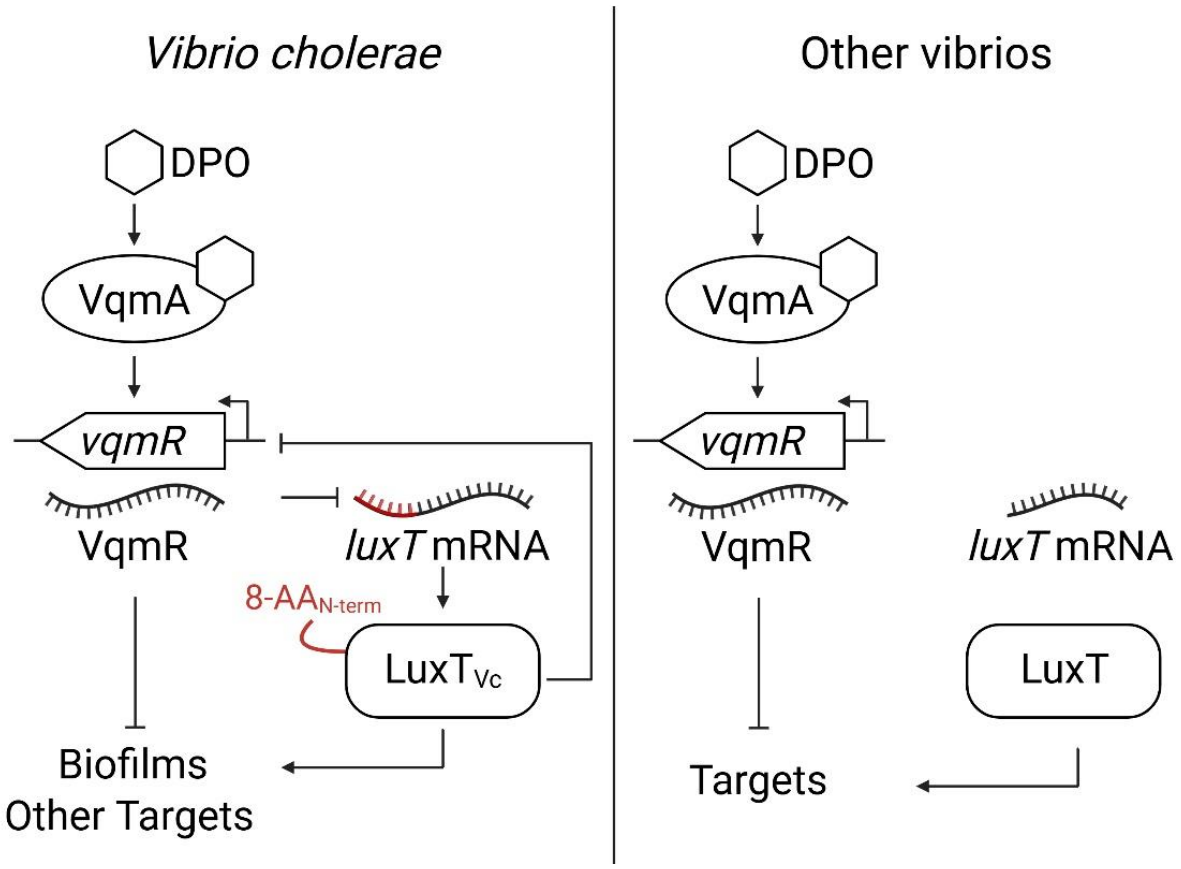

Figure 1. Simplified scheme for a double negative feedback loop comprised of the VqmR small RNA and the LuxT transcription factor. This regulatory loop exists in *V. cholerae* and closely related vibrios but not in more distant relatives. In the left panel, the designation 8-$AA_{N\text{-}term}$ on the LuxT protein and the red portion of the *luxT* mRNA show the regions required for the double negative feedback loop. See text for details.

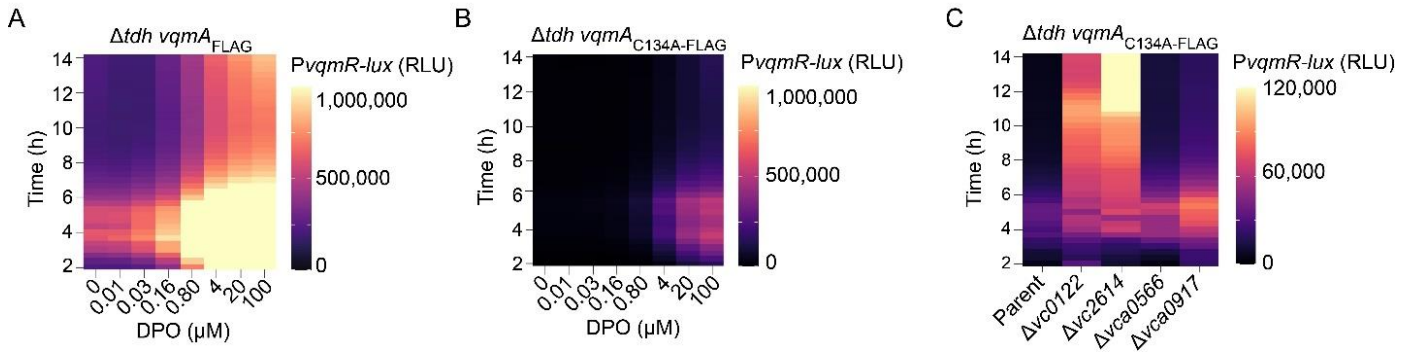

Figure 2. A genetic screen identifies repressors of the DPO-VqmA-VqmR QS circuit. (A) Light production over time from Δ*tdh vqmA*$_{FLAG}$ P*vqmR-lux* and (B) Δ*tdh vqmA*$_{C134A\text{-}FLAG}$ P*vqmR-lux V. cholerae* strains following administration of the specified concentrations of DPO. (C) As in panel B in the strain containing the additional designated deletions. DPO was added at 10 μM. Maximum fold-changes relative to that in the parent for Δ*vc0122*, Δ*vc2614*, Δ*vca0566*, and Δ*vca0917* were 9-fold at 11 h, 13.5-fold at 11 h 20 min, 2.8-fold at 17 h, and 3.3-fold at 14 h, respectively. RLU denotes relative light units, which are bioluminescence per OD_{600}. Scale bars represent color:intensity. Also see Supplementary Figure S1.

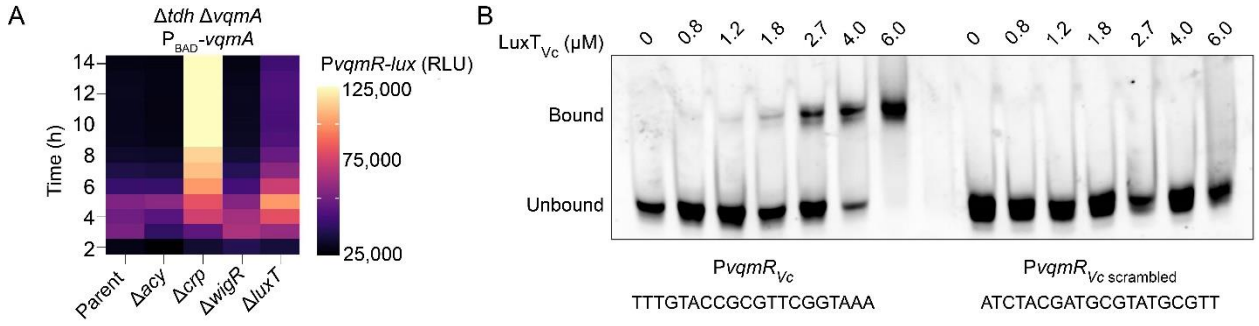

Figure 3. LuxT represses *vqmR* transcription. (A) Transcriptional output over time from P*vqmR-lux* following introduction of the indicated gene deletions in the Δ*tdh* Δ*vqmA* P_{BAD}-*vqmA V. cholerae* strain carrying P*vqmR-lux*. Maximum fold changes relative to the parent of the Δ*crp* and Δ*luxT* strains were 13.2-fold at 10 h and 2.5-fold at 8 h 20 min, respectively. (B) EMSA showing 6X-His-$LuxT_{Vc}$ (designated $LuxT_{Vc}$) binding to a P$vqmR_{Vc}$ probe (-111 to +49 relative to the $vqmR_{Vc}$ transcriptional start site) and the same probe with the putative LuxT binding site scrambled (P$vqmR_{Vc\ scrambled}$). The 20-nucleotide motif and its scrambled version are shown. All lanes contained 15 ng of promoter DNA. Bound and unbound DNA probes are designated.

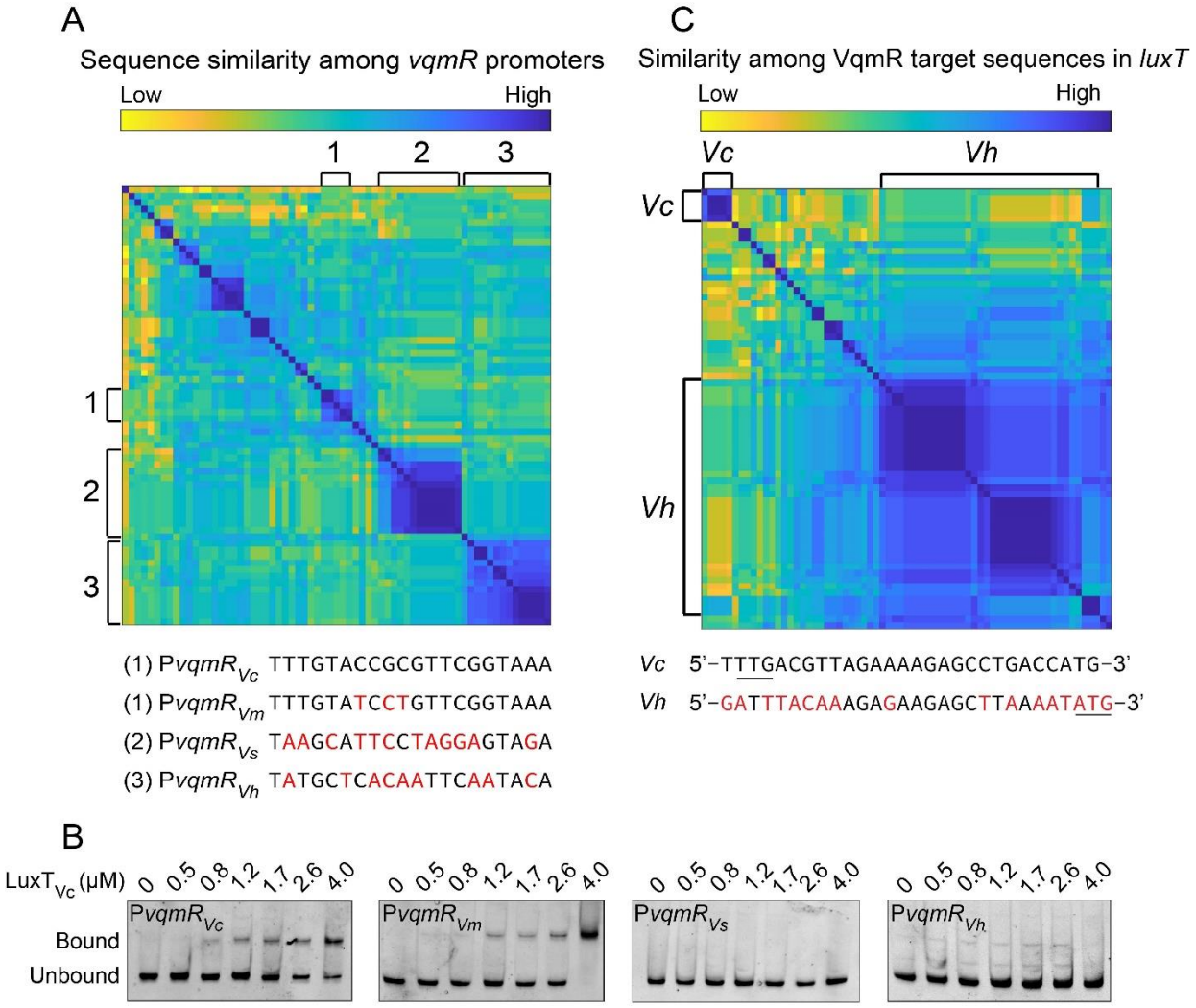

Figure 4. LuxT binds P*vqmR* in *V. cholerae* and in its close relative *V. metoecus*, but not P*vqmR* in more distantly related vibrios. (A) Pair-wise sequence similarity color-map of *vqmR* promoter regions from one representative genome from sixty-three vibrio species that harbor both *luxT* and *vqmR*. Hierarchical clustering was performed using the UPGMA algorithm (Unweighted Pair Group Methods with Arithmetic Mean). Putative LuxT binding sites for the designated groups are displayed below the heatmap with red indicating differences from the *V. cholerae* sequence. (B) EMSA of 6X-His-LuxT$_{Vc}$ (designated LuxT$_{Vc}$) binding to P*vqmR* DNA probes, similar in length to that in Figure 3B, containing putative LuxT binding sequences from *V. cholerae* (P*vqmR*$_{Vc}$), *V. metoecus* (P*vqmR*$_{Vm}$), *V. splendidus* (P*vqmR*$_{Vs}$), and *V. harveyi* (P*vqmR*$_{Vh}$). (C) Heatmap showing pair-wise

sequence similarity of the *vqmR* target sites in the *luxT* transcript across the same genomes as in panel A. Hierarchical clustering was performed using the UPGMA algorithm. A *V. cholerae*-like group (*Vc*) and a *V. harveyi*-like group (*Vh*) are highlighted, with representative sequences from each group shown below the heatmap. Red indicates differences from the *V. cholerae* sequence. The predicted TTG (*V. cholerae*) and ATG (*V. harveyi*) start codons are underlined.

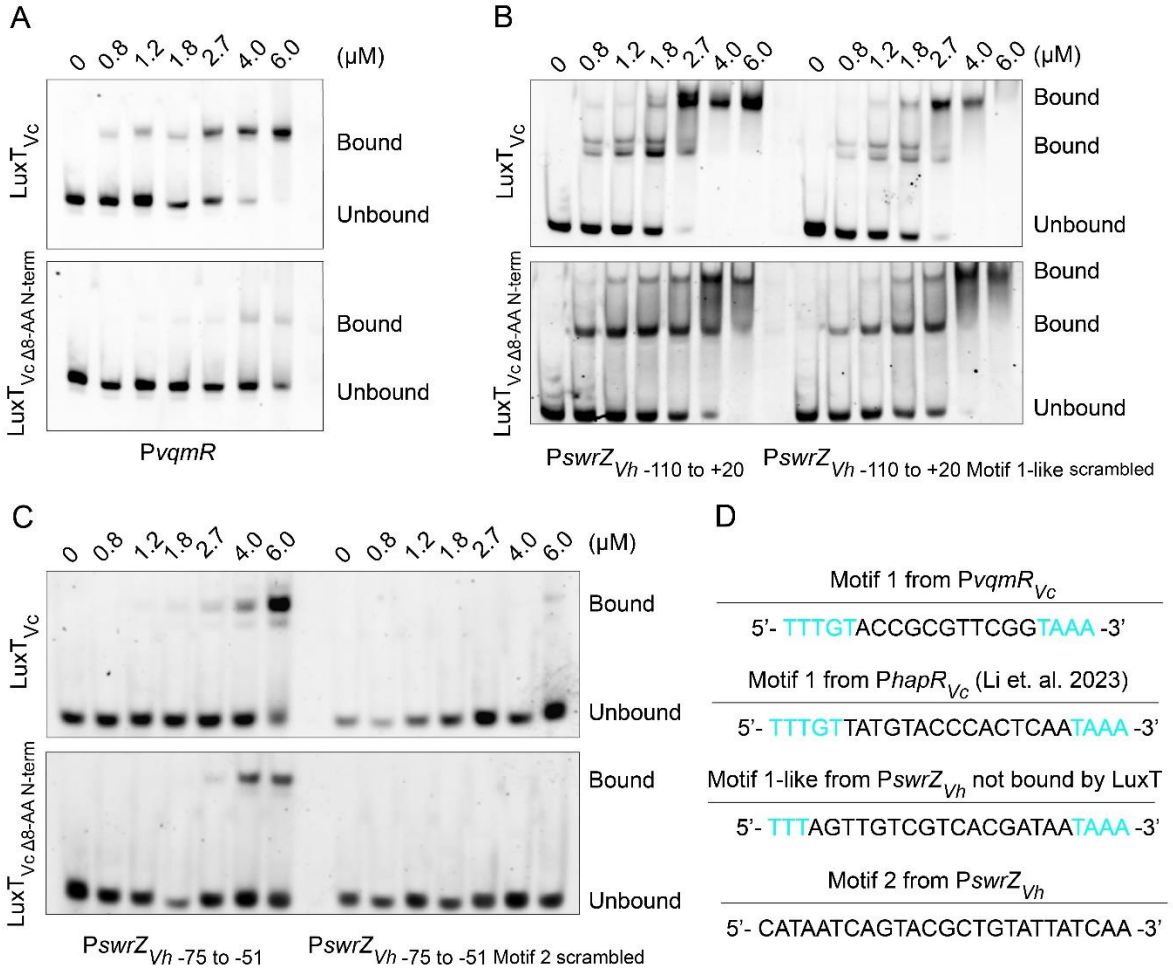

Figure 5. LuxT$_{Vc}$ binds distinct DNA motifs and the 8 N-terminal amino acids in LuxT govern which motif will be bound. (A-C) EMSA analyses for 6X-His-LuxT$_{Vc}$ and 6X-His-LuxT$_{Vc\ \Delta 8\text{-AA N-term}}$ (denoted LuxT$_{Vc}$ and LuxT$_{Vc\ \Delta 8\text{-AA N-term}}$, respectively) binding to the P*vqmR*$_{Vc}$ probe DNA or to probes for the designated *V. harveyi* P*swrZ*$_{Vh}$ regions. (D) Motifs identified as bound by LuxT in promoter regions of different genes. While writing this manuscript, a study by Li et. al. reported that the *V. cholerae hapR* promoter contains a Motif 1 site that is bound by LuxT$_{Vc}$ (41). In Motif 1, cyan represents conserved nucleotides. In panel B, left, the EMSA fragment denoted -110 to +20 contains both the Motif 1-like sequence and Motif 2. In panel B, right, the Motif 1-like sequence is scrambled. The probe in panel C contains only the Motif 2 sequence. Supplementary Figure 3 shows EMSAs with fragments containing only the Motif 1-like or only the Motif 2 sequence.

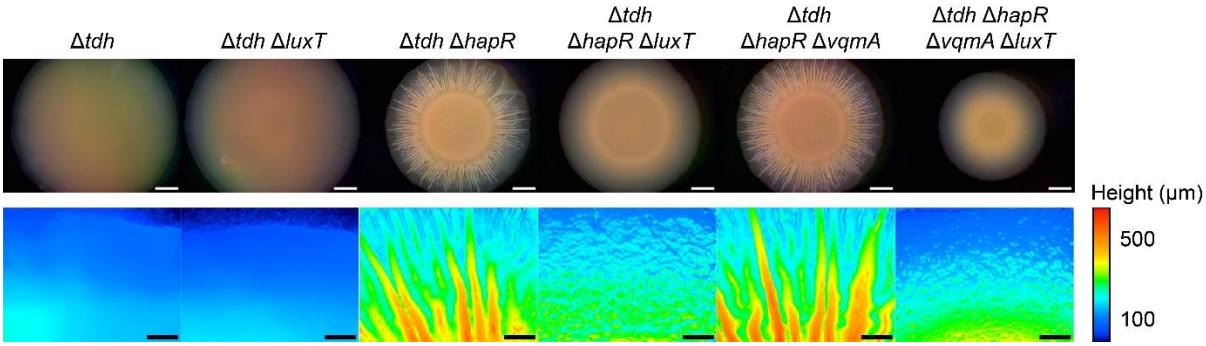

Figure 6. $LuxT_{Vc}$ promotes *V. cholerae* colony biofilm formation. Representative images of biofilms formed by the designated *V. cholerae* strains and companion 3D colony height profiles after 4 d. Height profiles are color mapped according to the scale provided.

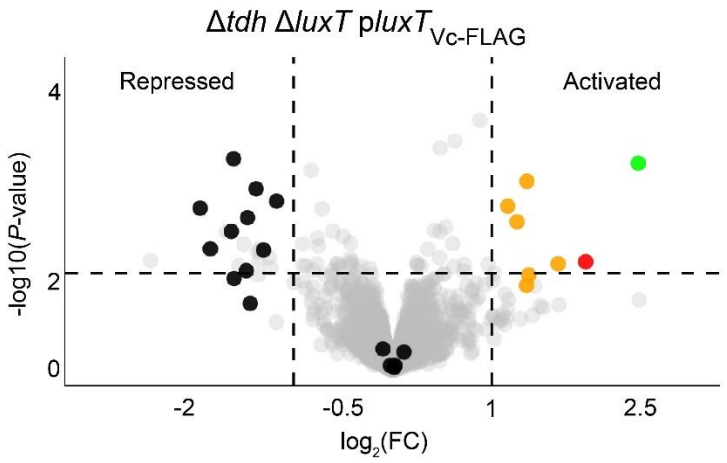

Figure 7. Transcriptomic analyses reveal the *V. cholerae* LuxT$_{Vc}$-controlled regulon. Volcano plot displaying gene expression patterns in the Δ*tdh* Δ*luxT V. cholerae* strain carrying *luxT$_{Vc}$* expressed from an arabinose inducible promoter with 0.1% arabinose. Sulfate metabolism genes are highlighted in black, galactose metabolism genes in orange, *vc1088* in red, and *luxT* in green. Data represent fold-changes for the indicated strain grown with 0.1% arabinose compared to the no arabinose condition. Genes repressed and activated by LuxT are denoted. The horizontal dotted line represents a P-value of 0.05. Left and right vertical dotted lines represent $\log_2$ fold-changes of −1 and 1, respectively. Samples are from n = 3 biological replicates. Complete datasets are provided in Dataset S1.

References:

1. Bassler BL. 1999. How bacteria talk to each other: regulation of gene expression by quorum sensing. Current Opinion in Microbiology 2:582–587.
2. Schauder S, Bassler BL. 2001. The languages of bacteria. Genes Dev 15:1468–1480.
3. Papenfort K, Bassler BL. 2016. Quorum sensing signal–response systems in Gram-negative bacteria. Nat Rev Microbiol 14:576–588.
4. Svenningsen SL, Waters CM, Bassler BL. 2008. A negative feedback loop involving small RNAs accelerates *Vibrio cholerae*'s transition out of quorum-sensing mode. Genes Dev 22:226–238.
5. van Kessel JC, Rutherford ST, Shao Y, Utria AF, Bassler BL. 2013. Individual and Combined Roles of the Master Regulators AphA and LuxR in Control of the *Vibrio harveyi* Quorum-Sensing Regulon. J Bacteriol 195:436–443.
6. Rutherford ST, van Kessel JC, Shao Y, Bassler BL. 2011. AphA and LuxR/HapR reciprocally control quorum sensing in vibrios. Genes Dev 25:397–408.
7. Mashruwala AA, Qin B, Bassler BL. 2022. Quorum-sensing- and type VI secretion-mediated spatiotemporal cell death drives genetic diversity in *Vibrio cholerae*. Cell 185:3966-3979.e13.
8. Shao Y, Bassler BL. 2014. Quorum regulatory small RNAs repress type VI secretion in *Vibrio cholerae*. Mol Microbiol 92:921–930.
9. Suckow G, Seitz P, Blokesch M. 2011. Quorum Sensing Contributes to Natural Transformation of *Vibrio cholerae* in a Species-Specific Manner ▿ . J Bacteriol 193:4914–4924.
10. Tsou AM, Frey EM, Hsiao A, Liu Z, Zhu J. 2008. Coordinated regulation of virulence by quorum sensing and motility pathways during the initial stages of *Vibrio cholerae* infection. Commun Integr Biol 1:42–44.
11. Hammer BK, Bassler BL. 2003. Quorum sensing controls biofilm formation in *Vibrio cholerae* : Biofilms in *Vibrio cholerae*. Molecular Microbiology 50:101–104.
12. Zhu J, Mekalanos JJ. 2003. Quorum Sensing-Dependent Biofilms Enhance Colonization in *Vibrio cholerae*. Developmental Cell 5:647–656.
13. Zhu J, Miller MB, Vance RE, Dziejman M, Bassler BL, Mekalanos JJ. 2002. Quorum-sensing regulators control virulence gene expression in *Vibrio cholerae*. Proc Natl Acad Sci USA 99:3129–3134.
14. Higgins DA, Pomianek ME, Kraml CM, Taylor RK, Semmelhack MF, Bassler BL. 2007. The major *Vibrio cholerae* autoinducer and its role in virulence factor production. Nature 450:883–886.
15. Bridges AA, Fei C, Bassler BL. 2020. Identification of signaling pathways, matrix-digestion enzymes, and motility components controlling *Vibrio cholerae* biofilm dispersal. Proc Natl Acad Sci U S A 117:32639–32647.
16. Bridges AA, Bassler BL. 2019. The intragenus and interspecies quorum-sensing autoinducers exert distinct control over *Vibrio cholerae* biofilm formation and dispersal. PLoS Biol 17:e3000429.
17. Miller MB, Skorupski K, Lenz DH, Taylor RK, Bassler BL. 2002. Parallel Quorum Sensing Systems Converge to Regulate Virulence in *Vibrio cholerae*. Cell 110:303–314.

18. Papenfort K, Silpe JE, Schramma KR, Cong J-P, Seyedsayamdost MR, Bassler BL. 2017. A *Vibrio cholerae* autoinducer–receptor pair that controls biofilm formation. Nat Chem Biol 13:551–557.
19. Chen X, Schauder S, Potier N, Van Dorsselaer A, Pelczer I, Bassler BL, Hughson FM. 2002. Structural identification of a bacterial quorum-sensing signal containing boron. Nature 415:545–549.
20. Jung SA, Chapman CA, Ng W-L. 2015. Quadruple Quorum-Sensing Inputs Control *Vibrio cholerae* Virulence and Maintain System Robustness. PLoS Pathog 11:e1004837.
21. Barrasso K, Watve S, Simpson CA, Geyman LJ, van Kessel JC, Ng W-L. 2020. Dual-function quorum-sensing systems in bacterial pathogens and symbionts. PLoS Pathog 16:e1008934.
22. Papenfort K, Förstner KU, Cong J-P, Sharma CM, Bassler BL. 2015. Differential RNA-seq of *Vibrio cholerae* identifies the VqmR small RNA as a regulator of biofilm formation. Proc Natl Acad Sci USA 112.
23. Mashruwala AA, Bassler BL. 2020. The *Vibrio cholerae* Quorum-Sensing Protein VqmA Integrates Cell Density, Environmental, and Host-Derived Cues into the Control of Virulence 11.
24. Liang W, Pascual-Montano A, Silva AJ, Benitez JA. 2007. The cyclic AMP receptor protein modulates quorum sensing, motility and multiple genes that affect intestinal colonization in *Vibrio cholerae*. Microbiology 153:2964–2975.
25. Liang W, Sultan SZ, Silva AJ, Benitez JA. 2008. Cyclic AMP post-transcriptionally regulates the biosynthesis of a major bacterial autoinducer to modulate the cell density required to activate quorum sensing. FEBS Letters 582:3744–3750.
26. Manneh-Roussel J, Haycocks JRJ, Magán A, Perez-Soto N, Voelz K, Camilli A, Krachler A-M, Grainger DC. 2018. cAMP Receptor Protein Controls Vibrio cholerae Gene Expression in Response to Host Colonization. mBio 9:e00966-18.
27. Dörr T, Alvarez L, Delgado F, Davis BM, Cava F, Waldor MK. 2016. A cell wall damage response mediated by a sensor kinase/response regulator pair enables beta-lactam tolerance. Proc Natl Acad Sci USA 113:404–409.
28. Cheng AT, Ottemann KM, Yildiz FH. 2015. *Vibrio cholerae* Response Regulator VxrB Controls Colonization and Regulates the Type VI Secretion System. PLoS Pathog 11:e1004933.
29. Eickhoff MJ, Fei C, Cong J-P, Bassler BL. 2022. LuxT Is a Global Regulator of Low-Cell-Density Behaviors, Including Type III Secretion, Siderophore Production, and Aerolysin Production, in *Vibrio harveyi* 13.
30. Waters CM, Lu W, Rabinowitz JD, Bassler BL. 2008. Quorum Sensing Controls Biofilm Formation in *Vibrio cholerae* through Modulation of Cyclic Di-GMP Levels and Repression of *vpsT*. J Bacteriol 190:2527–2536.
31. Krasteva PV, Fong JCN, Shikuma NJ, Beyhan S, Navarro MVAS, Yildiz FH, Sondermann H. 2010. *Vibrio cholerae* VpsT Regulates Matrix Production and Motility by Directly Sensing Cyclic di-GMP. Science 327:866–868.
32. Yan J, Fei C, Mao S, Moreau A, Wingreen NS, Košmrlj A, Stone HA, Bassler BL. 2019. Mechanical instability and interfacial energy drive biofilm morphogenesis. eLife 8:e43920.

33. Casper-Lindley C, Yildiz FH. 2004. VpsT is a transcriptional regulator required for expression of vps biosynthesis genes and the development of rugose colonial morphology in *Vibrio cholerae* O1 El Tor. J Bacteriol 186:1574–1578.
34. Fong JCN, Karplus K, Schoolnik GK, Yildiz FH. 2006. Identification and characterization of RbmA, a novel protein required for the development of rugose colony morphology and biofilm structure in *Vibrio cholerae*. J Bacteriol 188:1049–1059.
35. Fong JCN, Yildiz FH. 2007. The *rbmBCDEF* gene cluster modulates development of rugose colony morphology and biofilm formation in *Vibrio cholerae*. J Bacteriol 189:2319–2330.
36. Plate L, Marletta MA. 2012. Nitric oxide modulates bacterial biofilm formation through a multi-component cyclic-di-GMP signaling network. Mol Cell 46:449–460.
37. Anantharaman S, Guercio D, Mendoza AG, Withorn JM, Boon EM. 2023. Negative regulation of biofilm formation by Nitric Oxide Sensing Proteins. Biochem Soc Trans 51:1447–1458.
38. Hossain S, Heckler I, Boon EM. 2018. Discovery of a Nitric Oxide Responsive Quorum Sensing Circuit in *Vibrio cholerae*. ACS Chem Biol 13:1964–1969.
39. Cuthbertson L, Nodwell JR. 2013. The TetR Family of Regulators. Microbiol Mol Biol Rev 77:440–475.
40. Eickhoff MJ, Fei C, Huang X, Bassler BL. 2021. LuxT controls specific quorum-sensing-regulated behaviors in Vibrionaceae spp. via repression of qrr1, encoding a small regulatory RNA. PLoS Genet 17:e1009336.
41. Li Y, Yan J, Li J, Xue X, Wang Y, Cao B. 2023. A novel quorum sensing regulator LuxT contributes to the virulence of *Vibrio cholerae*. Virulence 14:2274640.
42. Lee S, Lewis DEA, Adhya S. 2018. The Developmental Switch in Bacteriophage λ: A Critical Role of the Cro Protein. J Mol Biol 430:58–68.
43. García-Tomsig NI, García-Rodriguez FM, Guedes-García SK, Millán V, Becker A, Robledo M, Jiménez-Zurdo JI. 2023. A double-negative feedback loop between NtrBC and a small RNA rewires nitrogen metabolism in legume symbionts. mBio 14:e0200323.
44. Herzog R, Peschek N, Fröhlich KS, Schumacher K, Papenfort K. 2019. Three autoinducer molecules act in concert to control virulence gene expression in *Vibrio cholerae*. Nucleic Acids Research 47:3171–3183.
45. Mashruwala AA, Bassler BL. 2024. Quorum sensing orchestrates parallel cell death pathways in *Vibrio cholerae* via Type 6 secretion-dependent and -independent mechanisms. Proc Natl Acad Sci U S A 121:e2412642121.
46. Vidakovic L, Mikhaleva S, Jeckel H, Nisnevich V, Strenger K, Neuhaus K, Raveendran K, Ben-Moshe NB, Aznaourova M, Nosho K, Drescher A, Schmeck B, Schulte LN, Persat A, Avraham R, Drescher K. 2023. Biofilm formation on human immune cells is a multicellular predation strategy of *Vibrio cholerae*. Cell 186:2690-2704.e20.
47. Gallego-Hernandez AL, DePas WH, Park JH, Teschler JK, Hartmann R, Jeckel H, Drescher K, Beyhan S, Newman DK, Yildiz FH. 2020. Upregulation of virulence genes promotes *Vibrio cholerae* biofilm hyperinfectivity. Proceedings of the National Academy of Sciences 117:11010–11017.

48. Conner JG, Teschler JK, Jones CJ, Yildiz FH. 2016. Staying Alive: *Vibrio cholerae* 's Cycle of Environmental Survival, Transmission, and Dissemination. Microbiol Spectr 4:4.2.02.
49. Dalia AB, McDonough E, Camilli A. 2014. Multiplex genome editing by natural transformation. Proc Natl Acad Sci USA 111:8937–8942.
50.Joska TM, Mashruwala A, Boyd JM, Belden WJ. 2014. A universal cloning method based on yeast homologous recombination that is simple, efficient, and versatile. Journal of Microbiological Methods 100:46–51.
51. Duddy OP, Silpe JE, Fei C, Bassler BL. 2023. Natural silencing of quorum-sensing activity protects *Vibrio parahaemolyticus* from lysis by an autoinducer-detecting phage. PLOS Genetics 19:e1010809.